Title: Use of Recycled Rubber Inclusions with Granular Waste for Enhanced Track Performance

Authors:

***Buddhima Indraratna** *PhD, FTSE, FIEAust, FASCE, FGS,*
Distinguished Professor of Civil Engineering, Founding Director of Australian Research Council's Industrial Transformation Training Centre for Advanced Technologies in Rail Track Infrastructure (ITTC-Rail), Director of Transport Research Centre, School of Civil and Environmental Engineering, University of Technology Sydney, Sydney, NSW 2007, Australia.
Email: buddhima.indraratna@uts.edu.au

Yujie Qi *PhD, AMASCE,*
Lecturer, and Program Co-leader of Transport Research Centre, School of Civil and Environmental Engineering, University of Technology Sydney, Sydney NSW 2007, Australia. Email: yujie.qi@uts.edu.au

Chamindi Jayasuriya *PhD,*
Senior Technical Support Officer, Faculty of Engineering and Information Technology, University of Technology Sydney, Sydney NSW 2007, Australia. Email: Chamindi.Jayasuriya@uts.edu.au

Cholachat Rujikiatkamjorn PhD, MASCE,
Professor, Transport Research Centre, School of Civil and Environmental Engineering, University of Technology Sydney, Ultimo, NSW 2007, Australia.
Email: cholachat.rujikiatkamjorn@uts.edu.au

Chathuri M. K. Arachchige *BSc (Hons)*
PhD Candidate, Transport Research Centre, University of Technology Sydney, NSW 2007. Australia. Email: chathuri.arachchige@student.uts.edu.au

***Author for correspondence:**
Distinguished Prof. Buddhima Indraratna
School of Civil and Environmental Engineering,
Faculty of Engineering and Information Technology,
University of Technology Sydney,
Sydney NSW 2007, AUSTRALIA
Ph: +61 2 4221 3046, Email: buddhima.indraratna@uts.edu.au

Abstract: The application of recycling waste materials such as coal wash (CW), steel furnace slag (SFS), and recycled tyre products in transport infrastructure developments is an efficient way of minimising waste accumulation in stockpiles. Apart from significant economic and environmental benefits, it helps to improve the stability and longevity of infrastructure foundations. This paper presents two of the recent novel studies on (i) a synthetic energy absorbing layer (SEAL) by mixing SFS, CW and recycled rubber crumbs (RC) for railway subballast, and (ii) under sleeper pads (USPs) to increase track stability and reduce ballast degradation. The track performance incorporating SEAL with different rubber contents and USP with various stiffnesses was investigated using large-scale laboratory tests and numerical modelling. The test results and the numerical simulation indicate that the inclusion of USP acts as an energy absorber and reduces the deformation and ballast degradation; the SEAL with 10% rubber can efficiently reduce the lateral dilation and ballast breakage and increase the energy dissipation with an acceptable level of settlement.

Keywords: railway tracks; under sleeper pads; rubber crumbs; ballast degradation; track stability

1. Introduction

Ballasted rail tracks are currently dominating the freight and passenger rail transport in Australia. However, track deterioration (e.g. ballast breakage, fouling, differential settlement, lateral instability) is one of the main factors leading to frequent and costly track maintenance. In the state of New South Wales (Australia) alone, replenishing ballast costs over $15 million/year causing significant environmental impact [1]. Moreover, due to the increasing demand on the travel and supply chains in the mining and agriculture sectors, the rail network is expected to operate under heavier loads and faster speed. Therefore, there is an emergent need to develop innovative solutions that can minimise ballast degradation, while controlling excess load propagation to the underlying subgrade layers.

Throughout the world, substantial volumes of end-of-life tyres are being accumulated in stockpiles in mining sites, landfills or illegally dumped while only a small proportion of rubber wastes is being recycled [2, 3]. Recycling these waste tyres in large-scale transportation infrastructures (e.g. railways) is one of the most efficient methods of reducing the large stockpiles on useful land, as well as providing an innovative solution to minise track degradation caused by high frequency dynamic load. For example, scraped tyres have been reformed into resilient rubber mats (e.g. under sleeper pads, under ballast mats) and installed in railways to reduce the ballast breakage and track vibration, and to increase the energy absorbing capacity of the rail track [4-9]. Furthermore, Indraratna et al. [10] investigated the use of recycled car tyres filled with recycled ballast in the capping layer and found that the rubber tyre inclusions help increase the confining pressure, reduce the lateral movement and ballast degradation. Additionally, granulated rubber particles derived from waste tyres mixed with ballast, subballast or other marginal materials is another kind of applications, that have been incorporated in rail tracks to improve the durability of track foundation and increase the ductility of the track [11-16].

On the other hand, annually, millions of tons of granular waste (e.g. plastics, glass, demolition waste and mining by-products) are generated in Australia every year. Researches have endeavored to recycle them in the large-scale transport infrastructure construction [17-19]. Mining by-products such as steel furnace slag (SFS) and coal wash (CW) are the most common waste produced in Australian mines and they have generated serious environmental concerns [20, 21]. To overcome the individual weaknesses of these mining wastes, such as the swelling potential of SFS and the brittle nature of CW, they are usually mixed with other materials (e.g. fly ash, cement, rubber crumbs) rather than being used directly for geotechnical applications [22-27]. One of the successful examples is the use of blended SFS and CW for port reclamation work proposed by Chiaro et al. [20]. A further improvement of the SFS and CW mixture was proposed by Indraratna et al. [28] by adding granulated rubber to improve the energy absorbing capacity and ductility of the mixtures for railway applications.

In this paper, two novel methods of using these waste materials in rail tracks were further investigated via large-scale laboratory testing: (i) developing a synthetic energy absorbing layer (SEAL) by mixing SFS, CW and granulated rubber in lieu of traditional subballast layer, and (ii) installing under sleeper pads (USPs) made of recycled tyres to reduce track foundation deterioration. Geotechnical performance (e.g. deformation, breakage, energy absorption capacity) of the track specimen using these applications was evaluated and discussed. Finite element modelling (FEM) was also developed to validate the laboratory testing of the track satabilised with USP on stiff subgrades.

2. Materials and large-scale test program

2.1 Materials

SEAL mixtures were composed of three granular waste materials, i.e. steel furnace slag (SFS), coal wash (CW) and rubber crumbs (RC), which were obtained from the steel manufacturing industry, coal mines, and waste tyres, respectively. The particle size distribution of the granular mixture is similar to the traditional subballast materials (Figure 1a), and the RC content is changed (i.e. 0, 10, 20, 30 and 40% by total weight) within the SEAL mixture. In the mixture, the blending ratio of SFS and CW was kept as 7:3, which is recommended by Indraratna et al. [28] and Qi et al. [29] based on the overall strength and swelling of the mixtures. The photo in Figure 1a shows the appearance of the mixture SEAL10 (the number after 'SEAL' denotes the RC content within the mixture). The basic geotechnical properties of SFS, CW, RC and SEAL mixtures can be found in Table 1.

Three types of commercially available USPs were used for this study (Figure 1b). The pads were made from polyurethane polymer and were 10mm thick but with different stiffness (Soft pad, stiffness k_u =0.1N/mm^{-3}; Medium, k_u =0.15 N/mm^{-3}; and Stiff pad, k_u= 0.22 N/mm^{-3}). The properties of the USPs used in these experiments are summarised in Table 2.

2.2 Laboratory testing preparation and testing procedure

Large-scale laboratory cyclic tests were conducted to examine the performance of the track specimen with SEAL or USP using the track process simulation apparatus (TPSA), as shown in Figure 2a. The test chamber's dimensions were 600 mm×800 mm in area and 600 mm high. For the testing program with SEAL, the specimen was composed of three layers: ballast layer on top (200 mm thick), structural fill layer at the bottom (100 mm thick), and the middle layer (150 mm thick) was either SEAL by changing RC contents (0, 10, 20, 30 and 40%) or traditional subballast materials (Figure 2b). Both ballast, traditional subballast and structural fill were obtained from a local quarry, and all of them were compacted (dry) to field conditions (dry densities: $\gamma_{d,ballast} = 15.4\ kN/m^3$), $\gamma_{d,subballast} = 18.5\ kN/m^3$,$\gamma_{d,stuctural\ fill} = 21.4\ kN/m^3$) and SEAL mixtures were compacted to 95% of their maximum dry density (20.3-12.4 kN/m^3 depending on rubber contents, Table 1) with their optimum moisture contents (5-12%, Table 1). For testing program with USP, to simulate a stiff subgrade condition such as bridges, tunnels, and road crossings, a concrete deck was used as the base of the test chamber (Figure 2d). The dimensions of the concrete block were selected in consonance with the plane area of the testing space and therefore the height, length, and width of the concrete base was 150 mm by 790 mm by 590 mm, respectively. On top of the concrete base, a 300 mm thick of fresh ballast was compacted by a vibratory compactor (to avoid any damage a rubber pad was attached to the vibration plate). For all the test specimens, settlement pegs and pressure plates were installed on top of each layer (ballast, subballast, subgrade/concrete base) to measure the displacements and pressures at the interfaces. Finally, a concrete sleeper ($200\times 680 \times 150\ mm$) with rail was placed on top of the ballast layer, and then the surrounding space between the sleeper and the chamber was filled with crib ballast. For USP, pads with different stiffness were glued underneath the sleeper in accordance with the specification provided by the USP supplier (Figure 2c), and then one test was also conducted without USP. To examine the pressure and the contact area at the interface of ballast-sleeper with and without USP, Matrix-based Tactile Surface Sensors (MBTSS; Figure 2e) were installed underneath the sleeper (Figure 2f). The MBTSS sensor (sensing area 500 ×200 mm) was calibrated using the linear multi-point calibration method before the testing.

The cyclic loads were applied with the maximum vertical stress of 230 kPa and a frequency of 15 Hz. This is to simulate a train with a 25 tonne axle load with a speed of 110 km/h [30]. The harmonic sinusoidal load was applied onto the sleeper rail assembly by the dynamic actuator. A strain control load was applied initially at a rate of 1 mm/sec, until the applied stress reached a mean cyclic stress $\sigma'_{cyc,mean}$. After that, the stress control load was applied in 2 phases consisted of a conditioning phase and a loading phase. In the conditioning phase, a low-frequency cyclic load (5 Hz) was applied for up to 100 cycles. This was to ensure the sleeper makes complete contact with the ballast to prevent any damage to the actuator. During the test, two sidewalls of the specimen chamber were fixed by applying an opposite load using hydraulic jacks, while the other two sidewalls (perpendicular to the sleeper) were subjected to lateral confinement of 15 kPa, and they were allowed to move. This was to simulate the plane strain condition assuming the deformation in the longitudinal direction of the track is negligible [31]. Each test was completed when the number of loading cycles reached N=500,000. After each test, the ballast directly under the sleeper was sieved to evaluate the ballast breakage. More detailed test preparation and procedure can be found in Qi and Indraratna [32], [3] and Jayasuriya et al. [4].

3. Laboratory testing results

3.1 Deformation behaviour

3.1.1 vertical and lateral deformation of SEAL

Figure 3 shows the deformation behaviour (settlement and lateral displacement) of the track specimen with and without SEAL. During the test, the specimen with SEAL40 collapsed within 1500 cycles due to severe vibration and excessive settlement (more than 40mm), while all other specimens were completed successfully to 500,000 cycles. As expected, by increasing RC contents in the SEAL the settlement of the track specimen increases from 7 mm (SEAL0) to 21 mm (SEAL30). This is due to the increasing compressibility of the rubber-soil mixtures by adding rubber [16, 33]. The vertical deformation of test specimens (excludes the one with SEAL40) increases with loading cycles and stabilizes with negligible strain accumulation rate (0.5×10^{-7} mm/mm/cycle) after 10,000 cycles. Noted that the lateral dilation of the track specimen was reduced by adding rubber in the SEAL (Figure 3b). However, when the RC content is more than 10% the lateral displacement tends to fluctuate, which may induce unstable track deformation when subjected to moving loads. Compared to the track specimen with traditional subballast materials tested by the current study and Navaratnarajah et al. [31] under the same loading conditions, the track specimen with SEAL0 and SEAL10 has comparable settlement, and the one having SEAL10 presents less lateral dilation, which is preferable to be used in rail tracks.

3.1.2 vertical and lateral deformation of USP with changing stiffness

Figures 4a and 4b show how the vertical and lateral deformations of ballast vary depending on the stiffness of the pads. In all four cases with and without USP, there is a rapid accumulation of plastic strain in the initial loading cycles (up to around 10,000 cycles), but then the rate of deformation decreases and the ballast stabilises after 100,000 cycles. When a dynamic load is applied, the particles are further compacted and rearranged, which can lead to significant plastic deformation. After several thousands of load cycles, the ballast is compacted to its optimum state and therefore the rate of strain accumulation decreases. Any further increase in permanent deformation is mainly caused by ballast breakage. According to Figures 4a and 4b, all three USPs can reduce the permanent lateral and vertical deformation, but the stiffer pads perform better than the softer pads. These results indicate only a certain type of USP can improve the longevity of ballast life with high efficiency. Figures 4c and 4d show the variations of the final total deformations (vertical and lateral) at the end of 500,000 cycles depending on pad stiffness. Stiff pads reduce the vertical and lateral deformations by approximately 50% comparing to the specimen without USP. The influence of USPs decreases with their stiffness. For soft pads, the vertical and lateral strains decrease by approximately 15% to 20%.

3.2 Ballast degradation

Ballast degradation is one of the main factors that govern the performance of the ballast layer. An ideal ballast layer should provide enough stability for sleepers to withstand the vertical and horizontal forces generated by rolling stock while facilitating the drainage with adequate permeability. Ballast degradation increases the percentage of fines in the ballast, which adversely affects permeability; this may further lead to track failure during heavy rainfall [34]. Ballast breakage is evaluated using the ballast breakage index (BBI) following Indraratna et al. [35]. The definition of BBI is shown in Figure 5a, where it is the ratio of the area enclosed by the arbitrary boundary of maximum breakage with the grading curves after and before the test.

BBI of the track specimen with SEAL and traditional subballast material is shown in Figure 5a. Note that the BBI of the track with SEAL0 is similar to the traditional track specimen, while when 10% rubber is included in SEAL, there is a significant drop (around 60%) in BBI. However, when more rubber (>10%) is included in SEAL, BBI only decreases marginally. This suggests 10% rubber in SEAL is enough to reduce the ballast breakage.

Variations of BBI with the stiffness of USP and the stiff subgrade condition are shown in Figure 5b. The results show that a stiff pad minimises ballast degradation most efficiently (40%). With the decrease in the pad stiffness, the BBI increases, and the extent of ballast breakage with a very soft USP is similar to the specimen having no USPs. Therefore, a stiff pad is an ideal choice for reducing the degradation of ballast on a concrete deck.

3.3 Contract area of using USP

The stress at the interface between sleeper and ballast is generally higher than the applied load because of the smaller contact area between the ballast aggregates and hard concrete sleeper surface, hence causing more ballast breakage. Therefore, it is imperative to investigate how the inclusion of USP can affect the contact area and the pressure at the interface using matrix-based Tactile Surface Sensors (MBTSS).

The contact area and pressure at the sleeper-ballast interface under a 25-tonne axle load and with and without USP were shown in Figure 6. The high-stress concentration points which directly affect the durability of particles are visible, and they can cause excessive particle breakage. The pressure contours from the MBTSS show that USPs significantly increase the contact area by 32%. This is because of aggregates penetrating USPs, which then leads to a large reduction in the contact stress. Moreover, the inclusion of USP improves the uniformity of stress distribution (Figure 6), hence reducing the ballast breakage as shown by Figure 5b.

3.4 Analysis of energy absorption

3.4.1 Energy absorption of SEAL

During loading, the track specimen absorbs the energy input from the cyclic loading, the absorbed energy can be partially dissipated via plastic deformation, particle breakage (mainly ballast), and in other forms of energy (e.g. sound and heat), and part of the energy can be released via elastic deformation during unloading. The dissipated energy (E_d) during one loading cycle for a unit volume of the test specimen can be calculated through the area of the hysteretic loop, while the elastic energy ($E_{elastic}$) can be represented by the area under the unloading curve as shown in Figure 7. A summation of the dissipated energy and the elastic energy can be considered as the total absorbed energy by the test specimen.

Figure 7 shows the dissipated energy and elastic energy of the track specimen with changing RC contents in SEAL by the end of the test. It can be seen that the more RC in the SEAL mixture, the more energy is absorbed by the track specimen, indicating higher energy absorbing capacity of the SEAL. Noted that dissipated energy and elastic energy also increase as more rubber is included, albeit the track specimens with SEAL20 and SEAL30 have similar energy absorbing capacity. However, more dissipated energy indicates more deformation or ballast breakage, and more elastic energy can further induce elastic deformation causing more vibration [32, 36, 37]. When 40% RC is included there is a sharp increase in dissipated energy and elastic energy. This can result in a significant vibration and settlement observed during testing. From the test results of deformation and ballast breakage shown in Figures 3 and 5a, it can be concluded that when adding more rubber, the test specimen experiences more deformation but less ballast breakage, which means that the increased dissipated energy is mostly due to the deformation rather than particle breakage. An optimal RC content in SEAL should ensure the track has less ballast breakage with acceptable settlement and meanwhile not generate excessive vibration.

The dissipated energy of the track under stiff subgrade condition with and without USP is also shown in Figure 7. The inclusion of USP increases the dissipated energy of the track specimen. However, the increase in the USP stiffness decreases the capability of energy dissipation. As mentioned above, the dissipated energy is consumed in the form of particle breakage and plastic deformation. The increased deformation and ballast breakage with the decrease in USP stiffness shown in Figure 4 and Figure 5b explains the increase in the dissipated energy. The result indicates with a certain energy dissipating efficiency, stiffer pads can improve the longevity of ballast through the reduction of ballast degradation and deformation compared to the track without USP. This can reduce the frequency of track maintenance and lead to huge cost savings.

4. Numerical modelling for USP

The permanent vertical deformation of a unit cell of track on a stiff subgrade with and without USP was simulated via finite element modelling (FEM). The stress–strain behavior of a layered system consisting of a sleeper, ballast, and under-sleeper pad (USP) has been investigated using the finite-element method (FEM), for which the commercially available software ABAQUS was used. The three-dimensional FEM model developed in this study could simulate ballast behavior with and without a USP attached to the base of a concrete sleeper subjected to cyclic loading. The model described in the paper represents a plane strain condition by ensuring zero lateral strain in the longitudinal direction, which is realistic for a long straight track section. The FEM mesh structure consisted of 3D, 8-noded linear brick elements, i.e. reduced integration (C3D8R) hexahedral elements. The ballast and subballast were modelled as an elasto-plastic material adopting a non-associated flow criterions obeying the Drucker-Prager yield criterion [38]. This yield criterion has been particularly suitable to simulate free-draining coarse granular materials such as ballast, because its strength and yield characteristics depend mainly on the level of stress and the corresponding volumetric strain with no pore water pressure development [39, 40]. The boundary conditions in the physical model are comparable to real-life concrete sleepers although the sleeper length is considerably less. The test box dimensions were designed by exploiting double symmetry [41], and the pressure underneath the sleeper is similar to what we measure in track, i.e. 300-350 kPa. However, the laboratory test chamber only has a depth of 600mm, and as a result, the depth effect will have an influence on the stress distribution with depth especially if the subgrade is a thick soft soil. If the subgrade or capping layer is relatively shallow and very stiff (e.g. highly compacted sandy-gravel), or if the track is over a rock foundation or a concrete bridge deck (ie. zero displacement boundary) as the condition simulated in this study, then the boundary effects by the base steel plate of the test box will be not too dissimilar to the field conditions, the associated particle breakage computations will be realistic.

The simulation results of the ballast deformation were based on the track with traditional conditions or with USPs having varying stiffness (0.22 N/mm^3, 0.15 N/mm^3 and 0.1 N/mm^3). Materials parameters used for FEM are listed in Table 3. Figure 8 shows the predicted permanent vertical deformation of ballast with varying USP stiffness. The deformation contours show the variation of permanent vertical displacement in the ballast layer at the end of 10,000 cycles. The outcomes of FE analysis confirm the results of the experiments which is, with USP the vertical deformation of the ballast layer decreases and the stiffer pad performs better than relatively flexible pads in terms of reducing permanent deformation. The stiff pad reduces the vertical permanent deformation by 16%, and the impact of the USP decreases as stiffness of the pad reduces.

The predicted and measured permanent vertical deformations are plotted with the number of loading cycles in Figure 9. Note that the trend of the vertical deformations with the loading cycles are captured by the FEM simulation. The measured vertical deformations are higher than those from FEM due to ballast breakage which is not captured in the FE analysis. The FE predictions confirm that stiffer pad performs better than the relatively soft pads.

Noted that the inability of representing a substantial depth of the ground stratum is indeed a challenge when using most laboratory testing devices with a limited depth, hence the errors attributed to boundary effects will be inevitable. Given the dimensions of this process simulation test apparatus with a solid steel base at a depth of 600mm, the load distribution and deformation response of the physical model is still acceptable where a relatively stiff shallow subballast (e.g. compacted capping layer) is followed by a hard subgrade. If the subgrade is very soft and thick (e.g. estuarine clay in a low-lying floodplain), then the accuracy of the stress variation with depth will be compromised.

5. Conclusions

In this paper, two applications adopting recycled rubber products (i.e. under sleeper pads; and rubber crumbs) were introduced and discussed, including installing under sleeper pads (USPs) between the sleeper and ballast interface for stiff subgrade condition and replacing subballast layer using a synthetic energy layer (SEAL; mixtures of SFS, CW and RC). Large-scale laboratory tests were conducted to investigate the track performance incorporating USPs with different stiffness and SEAL mixtures with different rubber contents. FEM modelling was also established to verify the performance of the track specimen with and without USP. The following findings can be drawn from this paper:

- Using SEAL in lieu of traditional subballast reduced the lateral dilation of the track but increased the vertical deformation. When the rubber content was ≤ 10%, the vertical deformation was within the acceptable range comparing to the traditional track.
- When increasing rubber content to 10% in SEAL, the ballast breakage was reduced by 60%, but when more rubber was added in SEAL, no more benefit. This could be attributed to the increase in elastic energy of the track specimen. More rubber was included, more energy was dissipated, but more elastic energy was also generated and this caused more vibration. Therefore, 10% rubber is sufficient to be included in SEAL.
- SEAL10 is a proper waste mixture for subballast layer based on the overall test results, i.e. comparable settlement, less lateral dilation, and ballast breakage with acceptable vibration included by elastic energy.

- The incorporating of USPs reduced the vertical and lateral deformation of the track, reduced ballast breakage, and increased the energy dissipation, whereas the stiff USP performed better than the other softer USPs, which can significantly reduce the deformation (around 50%) and ballast degradation (40%) comparing to the track without USP.
- Installing USP increased the contact area between the sleeper and the ballast. This reduced the concentrated stress and increased the uniformity of stress distribution, hence reduced the ballast degradation.
- The numerical modelling verified the laboratory results (deformation) of the track specimen with and without USPs, and corroborated that the stiffer USP was the preferable choice to be installed in the track.

As the geotechnical property of the mining waste (SFS and CW) is highly dependent on the source origin, it is recommended to conduct sufficient laboratory tests before directly taking these mixtures into practice. Research on the SEAL mixtures by numerical modelling and field tests will be considered by the authors to further facilitate the application of these waste mixtures.

Acknowledgments

The authors wish to acknowledge the financial assistance provided by the Australian Research Council (ARC) Discovery Project (ARC-DP180101916), ARC Industry Linkage Project (LP200200915) and ARC Industry Transformation Training Centre for Advanced Rail Track Technologies (ARC-ITTC-Rail). The financial and technical assistance provided by various industry partners over the years including Australasian Centre for Rail Innovation (ACRI), RMS and Sydney Trains, c/o Transport for NSW, SMEC, Bestech, Douglas Partners, ASMS, South 32, Ecoflex Australia, Bridgestone, and Tyre Crumbs Australia) is gratefully acknowledged.

References

[1] Sydney-Trains, *Sydney Trains Annual Report*. 2014, Transport for NSW: Sydney Trains. 112.

[2] E. Mountjoy, D. Hasthanayake, and T. Freeman, Stocks & Fate of End of Life Tyres-2013-14 Study, National Environmental Protection Council (2015).

[3] Y. Qi and B. Indraratna, The Influence of Rubber Inclusion on the Dynamic Response of Rail Track, Journal of Materials in Civil Engineering (in press) (2021). https://doi.org/10.1061/(ASCE)MT.1943-5533.0004069

[4] C. Jayasuriya, B. Indraratna, and T.N. Ngo, Experimental study to examine the role of under sleeper pads for improved performance of ballast under cyclic loading, Transportation Geotechnics 19 (2019) 61-73.

[5] C. Kraśkiewicz, C. Lipko, M. Płudowska, W. Oleksiewicz, and A. Zbiciak, Static and dynamic characteristics of resilient mats for vibration isolation of railway tracks, Procedia Engineering 153 (2016) 317-324.

[6] S.K. Navaratnarajah and B. Indraratna, Use of rubber mats to improve the deformation and degradation behavior of rail ballast under cyclic loading, Journal of geotechnical and geoenvironmental engineering 143(6) (2017) 04017015.

[7] M. Sol-Sánchez, F. Moreno-Navarro, and M.C. Rubio-Gámez, Viability of using end-of-life tire pads as under sleeper pads in railway, Construction and Building Materials 64 (2014) 150-156.

[8] C. Ngamkhanong and S. Kaewunruen, Effects of under sleeper pads on dynamic responses of railway prestressed concrete sleepers subjected to high intensity impact loads, Engineering Structures 214 (2020) 110604.

[9] S. Kaewunruen, A. Aikawa, and A.M. Remennikov, Vibration attenuation at rail joints through under sleeper pads, Procedia engineering 189 (2017) 193-198.

[10] B. Indraratna, Q. Sun, A. Heitor, and J. Grant, Performance of rubber tire-confined capping layer under cyclic loading for railroad conditions, Journal of Materials in Civil Engineering 30(3) (2018) 06017021.

[11] B. Indraratna, Y. Qi, M. Tawk, A. Heitor, C. Rujikiatkamjorn, and S.K. Navaratnarajah, Advances in Ground Improvement Using Waste Materials for Transportation Infrastructure, Proceedings of the Institution of Civil Engineers-Ground Improvement (2020) 1-44.

[12] M. Sol-Sánchez, N. Thom, F. Moreno-Navarro, M. Rubio-Gamez, and G. Airey, A study into the use of crumb rubber in railway ballast, Construction and Building Materials 75 (2015) 19-24.

[13] Y. Qi, B. Indraratna, A. Heitor, and J.S. Vinod, Effect of rubber crumbs on the cyclic behavior of steel furnace slag and coal wash mixtures, Journal of Geotechnical and Geoenvironmental Engineering 144(2) (2018) 04017107.

[14] M. Koohmishi and A. Azarhoosh, Hydraulic conductivity of fresh railway ballast mixed with crumb rubber considering size and percentage of crumb rubber as well as aggregate gradation, Construction and Building Materials 241 (2020) 118133.

[15] M. Tawk, Y. Qi, B. Indraratna, C. Rujikiatkamjorn, and A. Heitor, Behavior of a Mixture of Coal Wash and Rubber Crumbs under Cyclic Loading, Journal of Materials in Civil Engineering 33(5) (2021) 04021054.

[16] H.-K. Kim and J.C. Santamarina, Sand–rubber mixtures (large rubber chips), Canadian Geotechnical Journal 45(10) (2008) 1457-1466.

[17] A. Arulrajah, F. Maghool, A. Mohammadinia, M. Mirzababaei, and S. Horpibulsuk, Wheel tracker testing of recycled concrete and tyre aggregates in Australia, Geotechnical Research 7(1) (2020) 49-57.

[18] E. Yaghoubi, N. Sudarsanan, and A. Arulrajah, Stress-strain response analysis of demolition wastes as aggregate base course of pavements, Transportation Geotechnics 30 (2021) 100599.

[19] A. Mohajerani, J. Vajna, T.H.H. Cheung, H. Kurmus, A. Arulrajah, and S. Horpibulsuk, Practical recycling applications of crushed waste glass in construction materials: A review, Construction and Building Materials 156 (2017) 443-467.

[20] G. Chiaro, B. Indraratna, S.A. Tasalloti, and C. Rujikiatkamjorn, Optimisation of coal wash–slag blend as a structural fill, Proceedings of the Institution of Civil Engineers-Ground Improvement 168(1) (2015) 33-44.

[21] G.Q. Lu and D.D. Do, Physical structure and adsorption properties of coal washery reject, Fuel 71(7) (1992) 809-813.

[22] M. Tüfekçi, A. Demirbaş, and H. Genc, Evaluation of steel furnace slags as cement additives, Cement and Concrete Research 27(11) (1997) 1713-1717.

[23] M. Khan, A. Castel, A. Akbarnezhad, S.J. Foster, and M. Smith, Utilisation of steel furnace slag coarse aggregate in a low calcium fly ash geopolymer concrete, Cement and Concrete Research 89 (2016) 220-229.

[24] Y. Qi, B. Indraratna, and M. Tawk. *Use of Recycled Rubber Elements in Track Stabilisation*. in *Geo-Congress 2020: Geo-Systems, Sustainability, Geoenvironmental Engineering, and Unsaturated Soil Mechanics*. 2020. American Society of Civil Engineers Reston, VA.

[25] A.S. Noureldin and R.S. McDaniel, Performance evaluation of steel furnace slag-natural sand asphalt surface mixtures (with discussion and closure), Journal of the Association of Asphalt Paving Technologists 59 (1990) 276-303.

[26] I.Z. Yildirim and M. Prezzi, Geotechnical properties of fresh and aged basic oxygen furnace steel slag, Journal of Materials in Civil Engineering 27(12) (2015) 04015046.

[27] Y. Xue, S. Wu, H. Hou, and J. Zha, Experimental investigation of basic oxygen furnace slag used as aggregate in asphalt mixture, Journal of hazardous materials 138(2) (2006) 261-268.

[28] B. Indraratna, Y. Qi, and A. Heitor, Evaluating the properties of mixtures of steel furnace slag, coal wash, and rubber crumbs used as subballast, Journal of Materials in Civil Engineering 30(1) (2018) 04017251.

[29] Y. Qi, B. Indraratna, A. Heitor, and J.S. Vinod, Closure to "Effect of Rubber Crumbs on the Cyclic Behavior of Steel Furnace Slag and Coal Wash Mixtures" by Yujie Qi, Buddhima Indraratna, Ana Heitor, and Jayan S. Vinod, Journal of Geotechnical and Geoenvironmental Engineering 145(1) (2019) 07018035.

[30] B. Indraratna, M.M. Biabani, and S. Nimbalkar, Behavior of geocell-reinforced subballast subjected to cyclic loading in plane-strain condition, Journal of Geotechnical and Geoenvironmental Engineering 141(1) (2015) 04014081.

[31] S.K. Navaratnarajah, B. Indraratna, and N.T. Ngo, Influence of under sleeper pads on ballast behavior under cyclic loading: experimental and numerical studies, Journal of Geotechnical and Geoenvironmental Engineering 144(9) (2018) 04018068.

[32] Y. Qi and B. Indraratna, Energy-Based Approach to Assess the Performance of a Granular Matrix Consisting of Recycled Rubber, Steel-Furnace Slag, and Coal Wash, Journal of Materials in Civil Engineering 32(7) (2020) 04020169.

[33] J. Fonseca, A. Riaz, J. Bernal-Sanchez, D. Barreto, J. McDougall, M. Miranda-Manzanares, A. Marinelli, and V. Dimitriadi, Particle–scale interactions and energy dissipation mechanisms in sand–rubber mixtures, Géotechnique Letters 9(4) (2019) 263-268.
[34] Y. Qian, H. Boler, M. Moaveni, E. Tutumluer, Y.M. Hashash, and J. Ghaboussi, Degradation-related changes in ballast gradation and aggregate particle morphology, Journal of Geotechnical and Geoenvironmental Engineering 143(8) (2017) 04017032.
[35] B. Indraratna, J. Lackenby, and D. Christie, Effect of confining pressure on the degradation of ballast under cyclic loading, Geotechnique 55(4) (2005) 325-328.
[36] D. Taborda, D. Potts, and L. Zdravković, On the assessment of energy dissipated through hysteresis in finite element analysis, Computers and Geotechnics 71 (2016) 180-194.
[37] W. Sas, A. Głuchowski, B. Bursa, and A. Szymański, Energy-based analysis of permanent strain behaviour of cohesive soil under cyclic loading, Acta Geophysica 65(2) (2017) 331-344.
[38] D.C. Drucker and W. Prager, Soil mechanics and plastic analysis or limit design, Quarterly of applied mathematics 10(2) (1952) 157-165.
[39] B. Leshchinsky and H.I. Ling, Numerical modeling of behavior of railway ballasted structure with geocell confinement, Geotextiles and Geomembranes 36 (2013) 33-43.
[40] M.M. Biabani, N.T. Ngo, and B. Indraratna, Performance evaluation of railway subballast stabilised with geocell based on pull-out testing, Geotextiles and Geomembranes 44(4) (2016) 579-591.
[41] B. Indraratna, W. Salim, and C. Rujikiatkamjorn, Advanced rail geotechnology-ballasted track: CRC press. 2011.

Table list

Table 1 General properties of SFS, CW, RC and SEAL mixtures

Table 2 Material properties for USP used in this study (modified after [4])

Table 3 Material properties for FEM

Table 1 General properties of SFS, CW, RC and SEAL mixtures

Materials	Specific gravity	Friction angle (°)	Maximum dry density (kN/m^3)	Optimum moisture content (%)
SFS	3.43	53.4	22.9	11.6
CW	2.11	36	17.2	9.8
RC	1.15	31	4.4	-
SEAL0	2.89	51.9	20.3	8.1
SEAL10	2.51	48.1	17.6	10.0
SEAL20	2.22	45.9	15.5	12.0
SEAL30	1.99	44.7	13.8	8.3
SEAL40	1.80	43.7	12.4	5.2

Table 2 Material properties for USP used in this study (modified after [4])

Material	: Polyurethane polymer		
Dimensions of the sleeper pads	: 200 mm x 680 mm		
Tear strength of the connection between the USP and concrete sleeper	: 0.5 N/mm^2		
USP No	**Thickness (mm)**	**Weight (N/m^3)**	**Static stiffness (N/mm^3)**
1	10	4200	0.22 (stiff)
2	10	4200	0.15 (medium soft)
3	10	5500	0.10 (soft)

Table 3 Material properties for FEM

Ballast			
Density	1560 kg/m^3		
Young's modulus	125 MPa		
Poisson's ratio	0.3		
Internal angle of friction	45°		
Angle of dilation	15°		
concrete			
Density	2400 kg/m^3		
Young's Modulus	36 GPa		
USP			
Density	420 kg/m^3	420 kg/m^3	550 kg/m^3
Stiffness	0.22 N/mm^3	0.15 N/mm^3	0.1 N/mm^3
Poisson's ratio	0.45	0.45	0.4
Damping coefficient	9.5×10^4 Ns/m	8.9 Ns/m	7.6 Ns/m

Figure captions

Figure 1. (a) Grading curves of SFS, CW and RC, and the SEAL mixtures with different RC contents; (b) USP with different stiffness used in this study.

Figure 2. (a) Track process simulation apparatus (TPSA), (b) cross-section view of the track specimen with SEAL; (c) Sleeper attached with USP; (d) cross-section view of the track specimen with USP; (e) Matrix-based Tactile Surface Sensors (MBTSS) controlling unit; and (f) track specimen with MBTSS sensor (modified after [4]).

Figure 3. Deformation behaviours of track specimen with SEAL (a) settlement; (b) lateral displacement (modified after [32]).

Figure 4. Variations of (a) vertical and (b) lateral deformation of track specimens with USPs, (c) final vertical and (d) lateral deformation of the track specimen at the end of the test with USPs (modified after [4]).

Figure 5 BBI of the track specimen (a) with SEAL with varying RC contents (b) with USPs with varying stiffness (data sourced from [4, 32]).

Figure 6. Contact area and pressure distribution between at the sleeper-ballast interface with and without USP.

Figure 7. Dissipated energy and elastic energy of the track specimen with SEAL mixtures and USPs with varying RC contents at the end of the test (data sourced from [4, 32]).

Figure 8. Numerical simulation of the vertical displacement of the track with and without USP.

Figure 9. FEM simulation and experimental results of vertical deformation of the track with and without USPs.

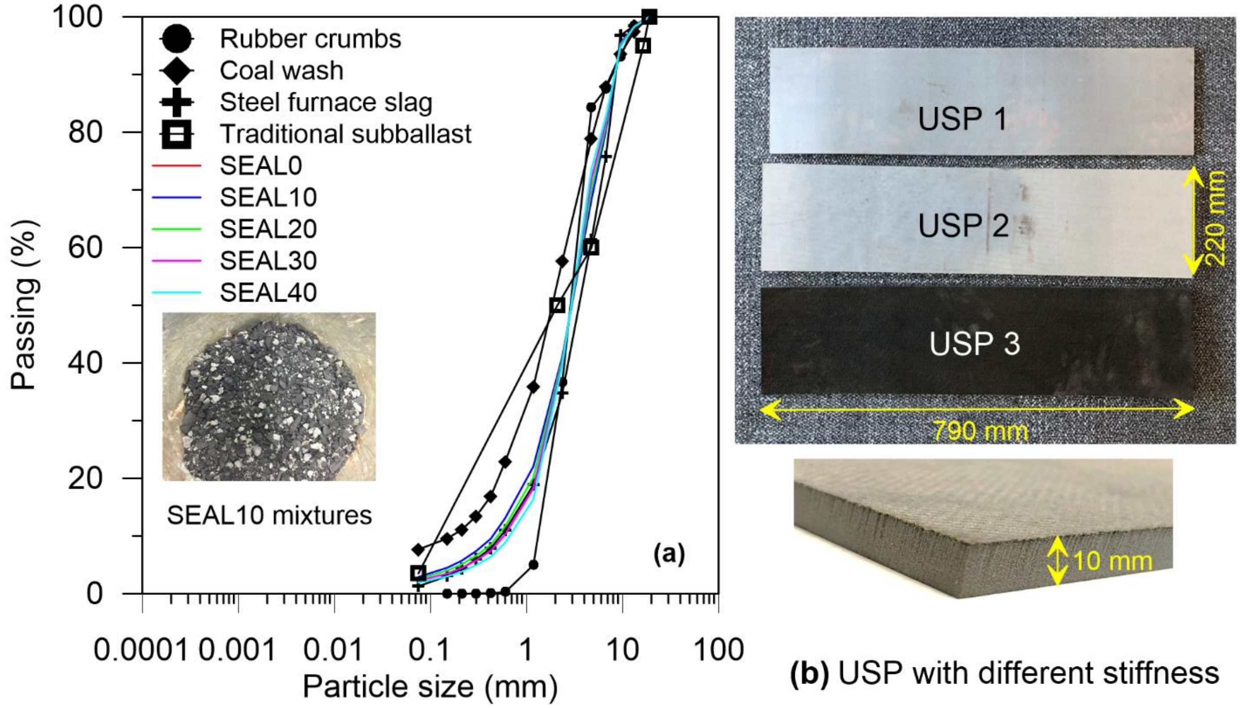

Figure 1. (a) Grading curves of SFS, CW and RC, and the SEAL mixtures with different RC contents; (b) USP with different stiffness used in this study.

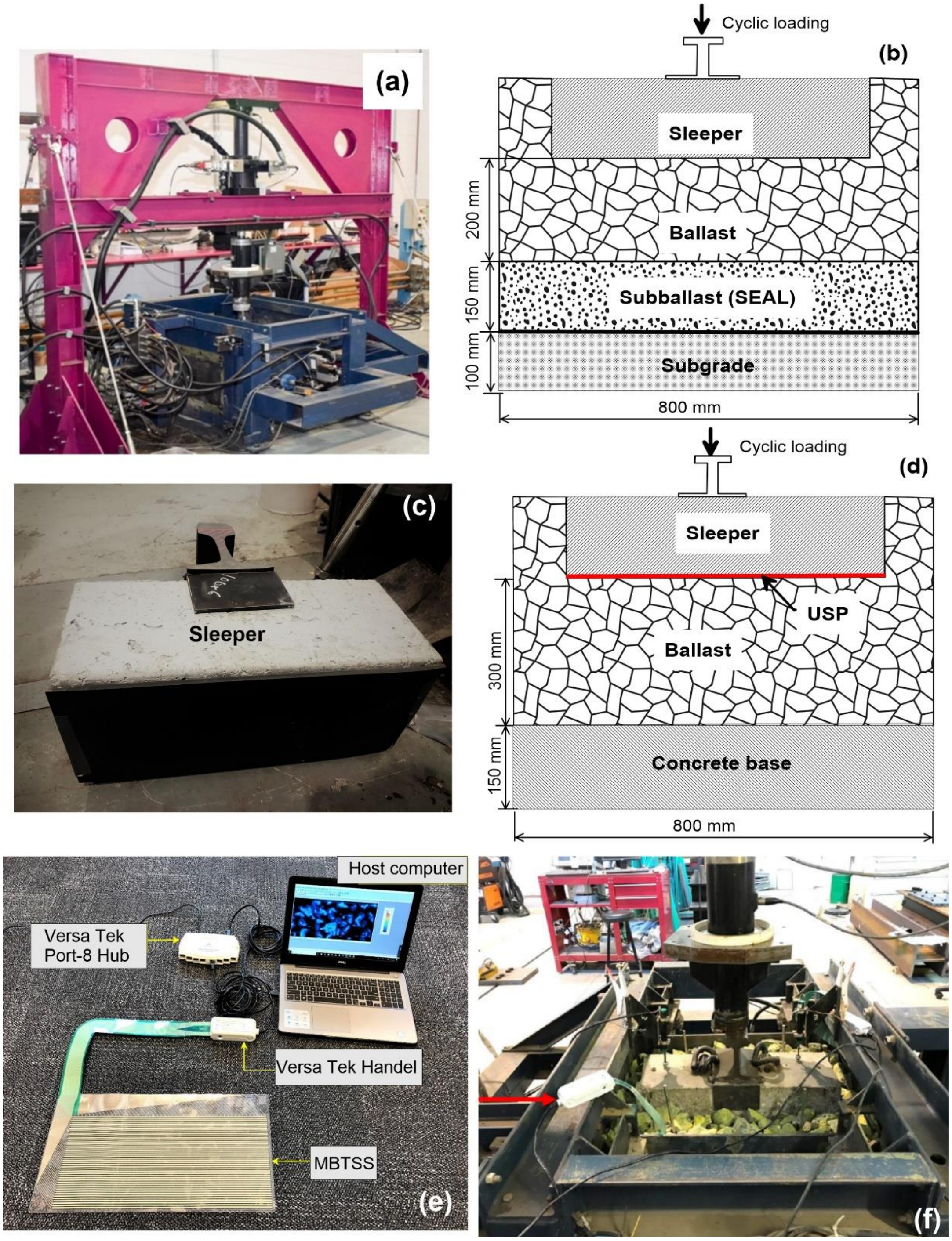

Figure 2. (a) Track process simulation apparatus (TPSA), (b) cross-section view of the track specimen with SEAL; (c) Sleeper attached with USP; (d) cross-section view of the track specimen with USP; (e) Matrix-based Tactile Surface Sensors (MBTSS) controlling unit; and (f) track specimen with MBTSS sensor (modified after [4]).

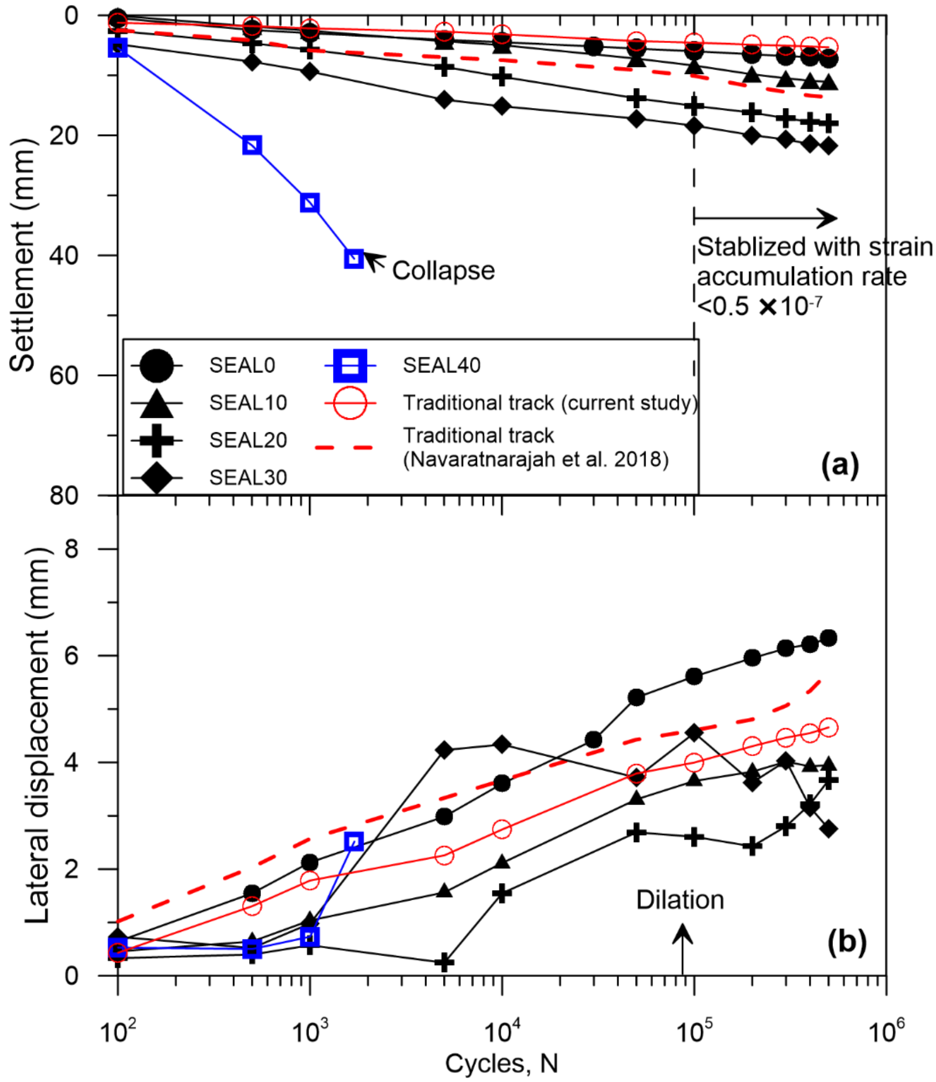

Figure 3. Deformation behaviours of track specimen with SEAL (a) settlement; (b) lateral displacement (modified after [32]).

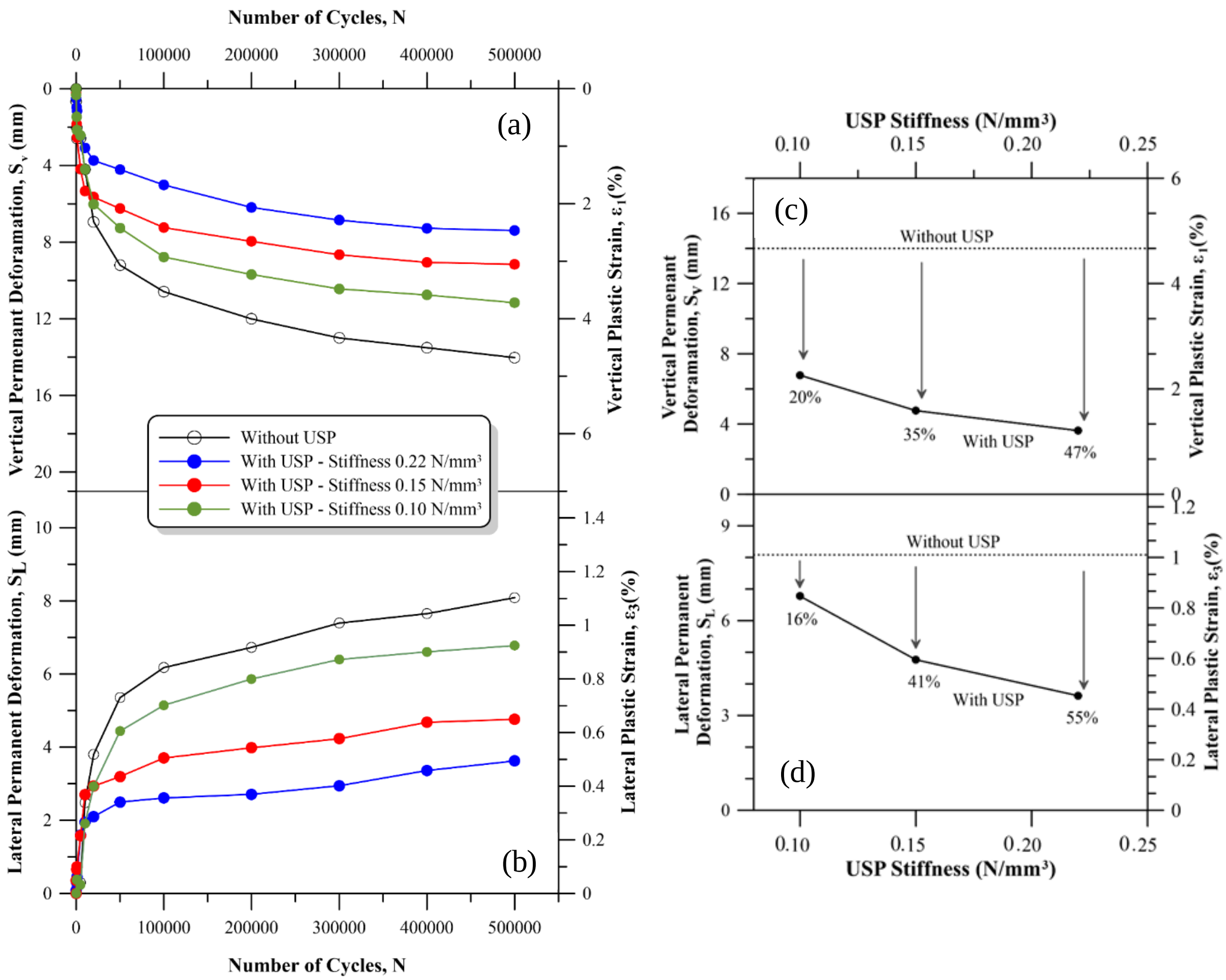

Figure 4. Variations of (a) vertical and (b) lateral deformation of track specimens with USPs, (c) final vertical and (d) lateral deformation of the track specimen at the end of the test with USPs (modified after [4]).

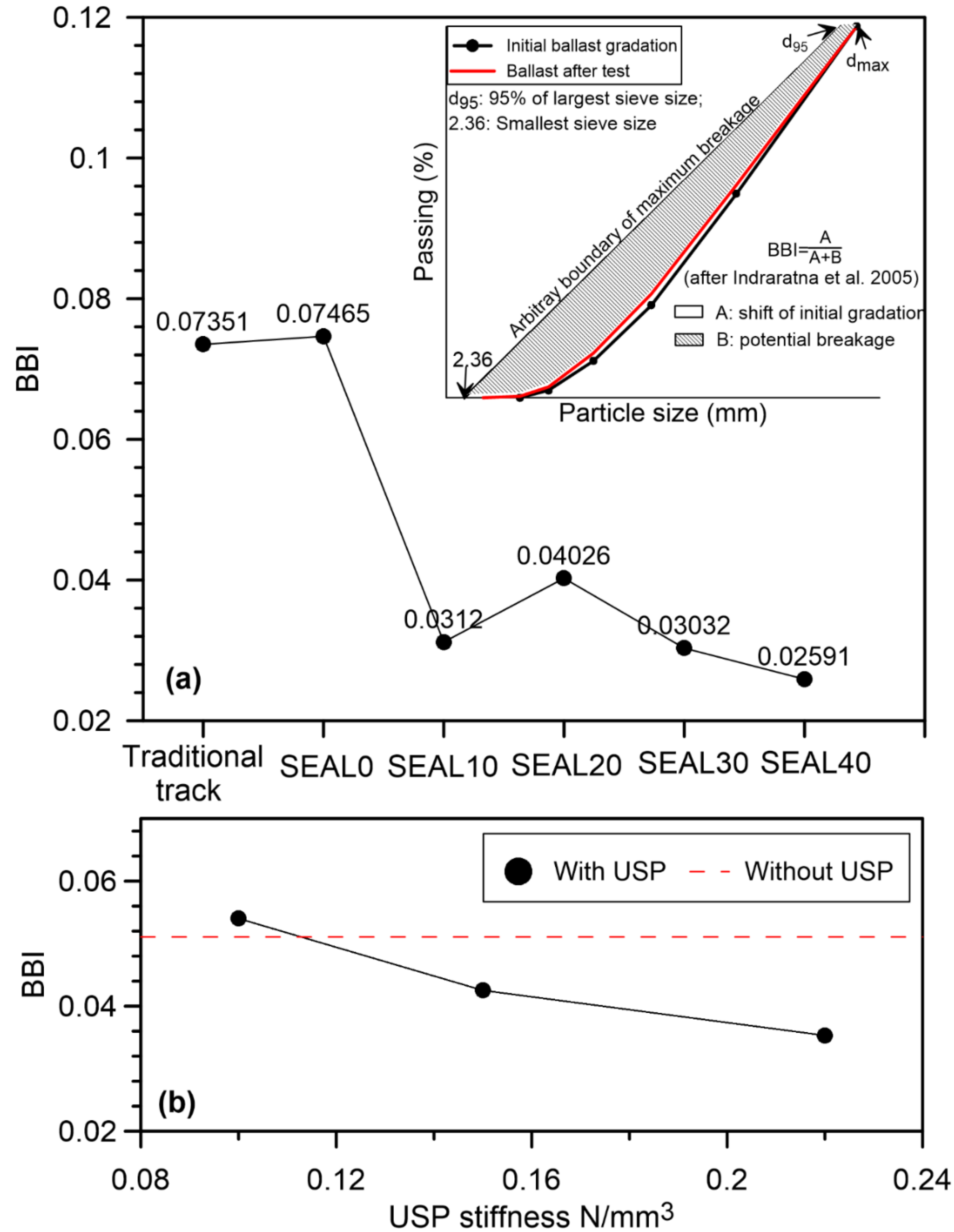

Figure 5 BBI of the track specimen (a) with SEAL with varying RC contents (b) with USPs with varying stiffness (data sourced from [4, 32]).

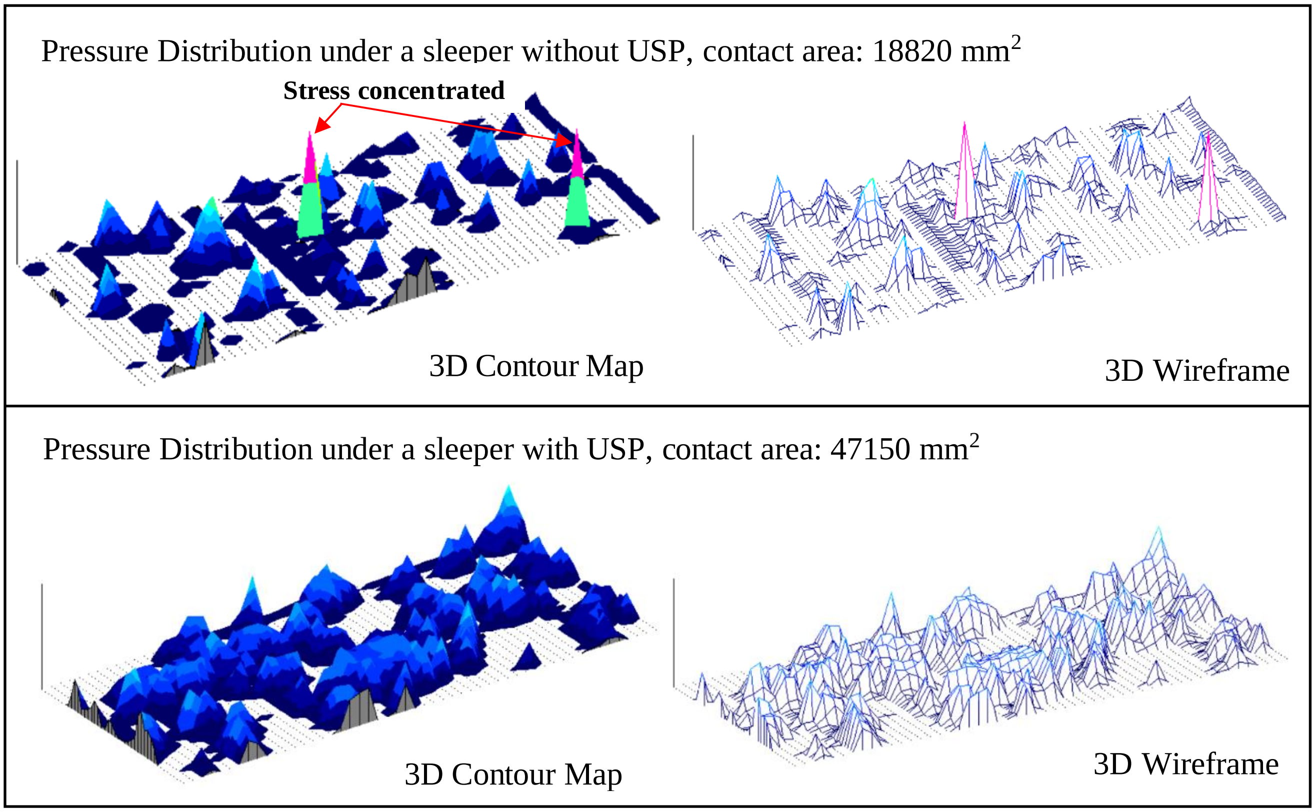

Figure 6. Contact area and pressure distribution between at the sleeper-ballast interface with and without USP.

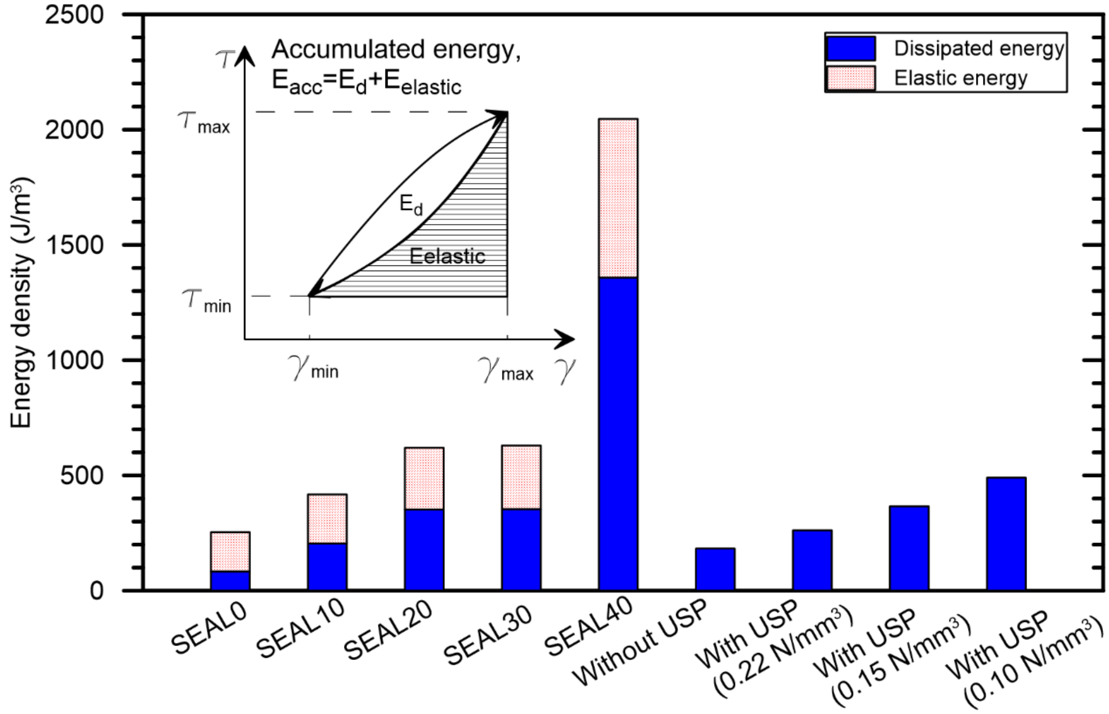

Figure 7. Dissipated energy and elastic energy of the track specimen with SEAL mixtures and USPs with varying RC contents at the end of the test (data sourced from [4, 32]).

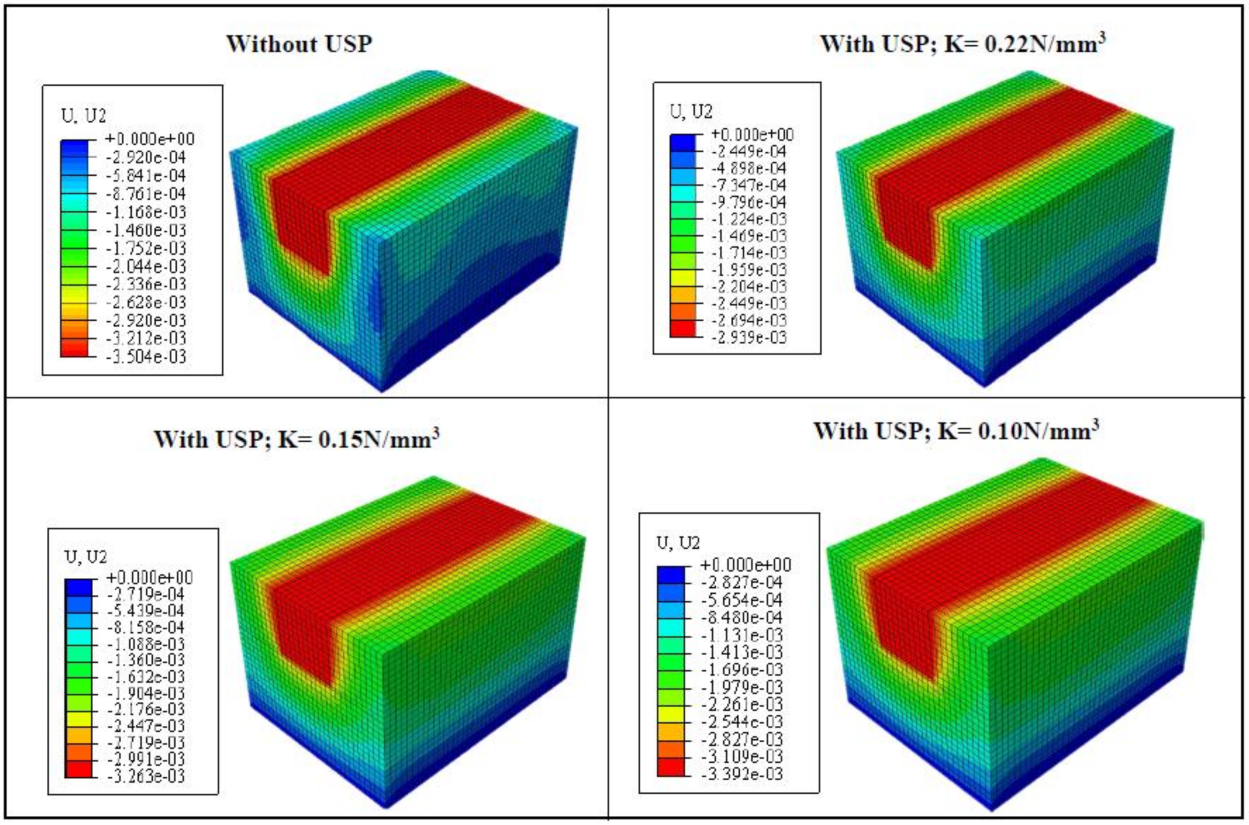

Figure 8. Numerical simulation of the vertical displacement of the track with and without USP.

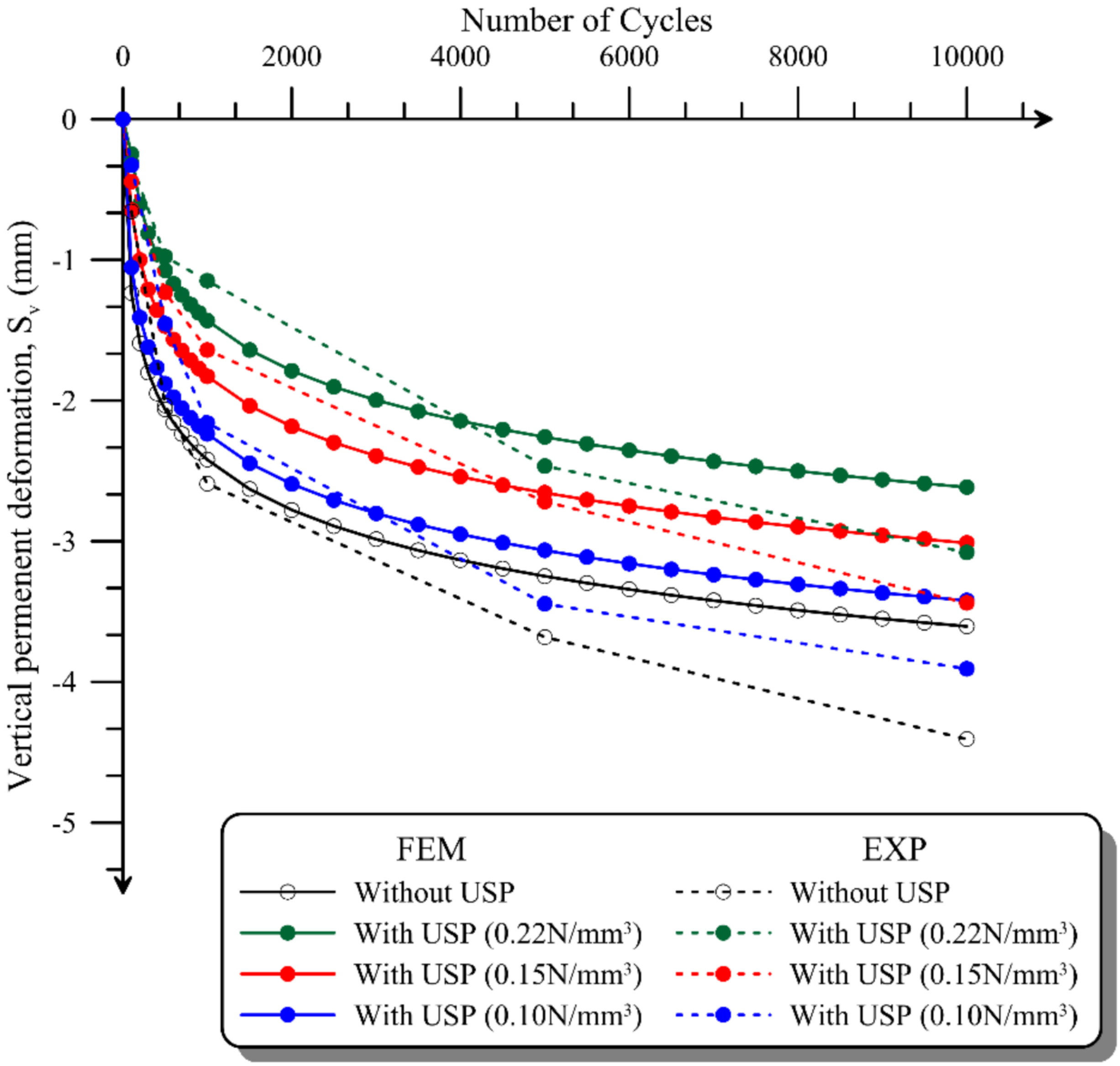

Figure 9. FEM simulation and experimental results of vertical deformation of the track with and without USPs.